ELSEVIER

Journal of Power Sources 63 (1996) 15–22

JOURNAL OF POWER SOURCES

The use of Hg/Hg_2SO_4 reference electrodes in valve-regulated lead/acid cells

Michael K. Carpente [a], Dawn M. Bernardi [a], John A. Wertz [1, b]

[a] *Physics and Physical Chemistry Department, Warren, MI 48090-9055, USA*

[b] *Manpower Technical Services, Southfield, MI 48034, USA*

Received 27 February 1996; revised 23 April 1996

Abstract

Reference electrode and gas flow measurements were used to characterize the discharge and charge behavior of a valve-regulated lead/acid cell. The implementation of a Hg/Hg_2SO_4 reference electrode suitable for this type of cell is described. The nature of the reference electrode gives rise to liquid-junction potentials. The liquid-junction potential theory is reviewed and applied to correct the measured half-cell potentials during cell operation. Corrections of over 60 mV were required for measurements at the end of discharge and beginning of charge. The PbO_2 electrode is shown to control the decrease in cell voltage during discharge; that is, discharge capacity is limited by the PbO_2 electrode. In contrast, during galvanostatic charge to a charge-voltage lid, the final cell voltage increase is controlled by the Pb electrode.

Keywords: Valve-regulated lead/acid batteries; Hg/Hg_2SO_4 reference electrodes; Gassing

1. Introduction

Much work has been done to characterize the behavior of the valve-regulated lead/acid (VRLA) battery under various conditions. A wide range of measurements, including battery and cell voltages, current, gassing rate, gas composition, internal pressure, and temperature, have been employed in these efforts [1–4]. One classical electrochemical measurement technique used for flooded batteries is the separate measurement of both PbO_2 and Pb electrode potentials versus an inserted reference electrode (RE). Information obtained from such measurements is typically the basis for determining at which electrode the limitation(s) to battery or cell performance occur under specific test conditions. Such information from VRLA batteries would be of particular interest; for example, while acid is typically the limiting discharge reactant on a stoichiometric basis, half-cell measurements using reference electrodes would make it possible to determine at which electrode the capacity-limiting phenomena actually occur. Analysis of half-cell potentials then should markedly improve our understanding of the limitations which determine discharge capacity and charge acceptance.

Unfortunately, the compact construction of many VRLA batteries is not compatible with the use of common RE designs. Each cell of a typical flat-plate VRLA battery design comprises a compressed stack of alternating PbO_2 and Pb pasted-plate electrodes separated by absorptive separators which are 1–2 mm thick, leaving little space for RE insertion. Furthermore, because all of the electrolyte is adsorbed within the plates and separators, there is no reservoir of free electrolyte in which to immerse an RE. Finally, since the battery is often not fully saturated with electrolyte, the use of an RE with a conventional Luggin capillary for long-term experiments is problematic since electrolyte would be drawn from the capillary into the undersaturated separator, thereby significantly affecting the physical conditions in the region of measurement.

Two approaches to providing a suitable RE for the VRLA system are the direct insertion of a mini (or micro) RE into the glass mat, and the use of an RE with a modified capillary connection. Reference electrodes suitable for the lead/acid system include Cd, Pb, Hg/Hg_2SO_4, and $PbO_2/PbSO_4$ [5,6]. Given these choices, the insertion of Cd or Pb wires as reference mini-electrodes initially seems appealing. However, the Cd electrode is not sufficiently stable for long-term measurements [2,5] while a Pb electrode would be susceptible to oxidation from oxygen generated within the system. The stability and relative ease of construction of the Hg/Hg_2SO_4 electrode have made it a popular choice for the lead/acid system [4,7], and we utilize it here with a modified capillary

[1] Current address: Trojan Battery Co., 12380 Clark, Santa Fe Springs, CA 90670, USA.

PII S0378-7753(96)02436-6

arrangement. The use of a $PbO_2/PbSO_4$ reference electrode in an experimental sealed lead/acid cell has also been reported [3]; however, keeping the PbO_2 charged presents a difficulty.

A key feature of the reference electrode described here is the modified capillary connection which drastically reduces electrolyte flow and diffusion from the saturated RE to the unsaturated VRLA environment. Therefore, during charge or discharge, while the concentration within the cell changes dramatically, the sulfuric acid concentration in the reference compartment remains essentially constant. The potential measurements made with the RE thus include a liquid-junction potential contribution, since the acid concentration in the RE can differ from that in the cell. We outline a method for treating the experimental data to account for the liquid-junction potential. Measurements taken with the reference electrode placed in a multi-plate VRLA cell are described and used to analyze some of the dynamics involved in the charge and discharge of the cell.

2. Experimental

The RE consists of a Hg/Hg_2SO_4 electrode of standard design in a small reservoir of sulfuric acid (7.50 *m* H_2SO_4). An outlet at the bottom of the reservoir was fitted with a 1–4 inch length of polyethylene tubing (internal diameter: 1/8 in). In the end of the tubing was fixed a short length (i.e., 1/4 in) of porous Vycor® glass (from Bioanalytical Systems, West Lafayette, IN, USA). It is through this porous Vycor® tip that solution contact is maintained between the reference electrode and the separator of a VRLA cell. The porous Vycor® was soaked in the sulfuric acid electrolyte for approximately 16 h prior to installation in the tubing. After installation, the tip was beveled on two sides with sandpaper to yield a chisel-like tip (see Fig. 1). Because the resulting RE has a relatively high impedance, a high impedance measurement circuit was required to obtain meaningful half-cell measurements. We used a Keithley Model 610B electrometer to condition the signal before collecting the data with a Genesis data-logging system from Iconics, Inc.

The VRLA cell, provided by the DELPHI Division of General Motors Corporation, was similar in design to cells in the electric vehicle battery currently under development at DELPHI [8]. The cell stack consisted of pasted-plate electrodes sandwiched between absorptive glass mat separators. The plates in the cell measured approximately (5–1/4) in × (3–1/4) in. The cell case included a one-way pressure vent. Measurements of gas flow from the vent were made with an electronic flow meter (Omega Engineering, Inc., Stamford, CT, USA), after first routing the gas through a drying tube filled with desiccant. A type-J thermocouple taped to the cell provided case-temperature measurements.

The RE was sealed into the cell case top after the porous Vycor® tip of the 'capillary' connection was first placed directly over a negative plate such that the separators on either side of the plate were contacted by the tip, as shown in Fig. 1. The RE tip was located 3.6 cm from the current collecting tab and 0.3 cm above the top of a Pb electrode plate. As discussed by Newman and Tiedemann [9], RE measurements are most meaningful when the exact position of the RE is specified. Since the ohmic potential losses between either electrode and the reference electrode tip should be negligible, changes in the measured half-cell potentials reflect primarily surface overpotentials of the electrochemical reactions with their corresponding concentration overpotentials.

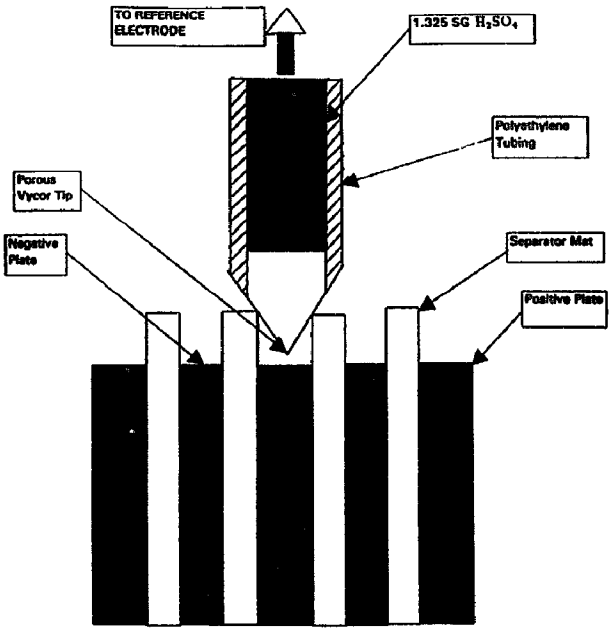

Fig. 1. Schematic showing a typical placement of the Vycor® tip of a reference in a cell. (Tip may actually straddle either a positive plate or a negative plate).

After the addition of the RE, the cell was repetitively cycled using a Bitrode® cycler under computer control. The cell was discharged at a rate of 12.7 mA/cm² to a cutoff voltage of 1.75 V. Following a 5 min rest, the cell was charged at a rate of 7.6 mA/cm² to a voltage lid of 2.5 V for 4 h. The cell was allowed to rest for 1 h before beginning the next discharge. Cell voltage, PbO_2 half-cell potential, case temperature, and the gas venting rate were continuously recorded for the duration of the test. The Pb half-cell potential was determined by difference (i.e., cell potential minus PbO_2 half-cell potential). The cell was cycled continuously, except for brief open-circuit stands.

The two major concerns regarding the long-term performance of the RE are the flow of electrolyte from the reference compartment to the undersaturated separator, and the diffusion of sulfuric acid between the RE and the cell. Since solution contact between the reference and cell must be maintained for continued RE operation, both processes are unavoidable. The role of the porous Vycor® tip in the RE is to minimize both processes. The tips' extremely small hydraulic permeability (i.e., 3×10^{-16} cm² [10]) would suggest that convective flow from the reference to the cell is not significant

Table 1
Values for liquid-junction potential calculation

Discharge current density, i	12.7 mA/cm²
Cell initial sulfuric acid concentration, m_A^o	6.1936 mol/kg
Reference sulfuric acid concentration, m_A^{RE}	7.496 mol/kg
Cell temperature, T	25 °C
Specific initial cell liquid volume, $\frac{V_l^o c_A^o}{A(N-1)}$	0.0107 cm³/cm²
Density of initial cell H_2SO_4 solution, ρ_l^o	1.280 g/cm³

— the average pore diameter of 50 Å results in a tremendous resistance to flow. Indeed, from monitoring the electrolyte level in the reference cell compartment of the RE mounted in the cell, the amount of electrolyte loss over the course of an extended cycling test (>3 months) was observed to be less than 1 ml. The diffusion of sulfuric acid, however, posed a bigger problem. While the acid concentration in the RE compartment was initially 7.5 *m*, after three months of cycling, the concentration had decreased to 6.3 *m*. This agrees with a rough estimate based on Fick's first law, of 0.5 to 3 months for the above acid concentration change in the RE compartment to occur. (We obtained this estimate by using the pore volume of 28% [10]; the lower bound of 0.5 months corresponds to a cell with pure water, while the upper bound of 3 months corresponds to a cell with the full charge acid concentration given in Table 1.) Clearly, over the course of a typical charge or discharge, the concentration change in the RE compartment would be insignificant. We have subsequently confirmed this with measurements of acid concentrations in a similar RE installed in a VRLA cell; we observed the change in acid concentration within the RE compartment to be a gradual one that can be neglected when analyzing the potential measurements for any one cycle. The concentration change occurring over many cycles, however, must be considered in the liquid-junction potential calculation — the concentration change of 7.5 to 6.3 *m* corresponds to approximately a 9 mV change in the liquid-junction potential. Calculations show that the change in acid concentration within the cell caused by this diffusion of sulfuric acid from the RE compartment is negligible.

3. Theoretical

The investigation of electrode potentials versus a reference electrode in VRLA cells requires consideration of liquid-junction potentials. A significant junction potential may arise since, typically, the acid composition within the RE remains constant during an experiment, while the acid composition in the cell may vary considerably. In the following section, we develop an equation to characterize the liquid-junction potential for concentrated aqueous H_2SO_4 solutions. We follow the general theories for a single electrolyte presented by Newman [11]. In the remaining sections, we discuss methods of applying this equation specifically to the VRLA system and interpreting experimental results.

3.1. Solution potential within a liquid-junction region

A liquid junction potential can be defined as the potential difference in the absence of current flow across a region of varying solution composition. In order to estimate the junction potential difference, one must choose a method of characterizing the potential in the solution within the junction. Let us define the solution potential with a Hg/Hg_2SO_4 electrode, and correspondingly, define the liquid-junction potential with the cell I:

$$|Hg|Hg_2SO_4|H_2SO_4^{\delta} \text{ in } H_2O|\text{junction}|H_2SO_4^{\epsilon} \text{ in } H_2O|Hg_2SO_4|Hg| \quad \text{I}$$

Using classical thermodynamics, we can write the cell potential E and therefore the junction potential E_j as

$$2FE = 2FE_j = \mu^{\delta}_{HSO_4^-} - \mu^{\epsilon}_{HSO_4^-} + \mu^{\epsilon}_{H^+} - \mu^{\delta}_{H^+} \quad (1)$$

With the relation

$$\mu_A = \mu_{H^+} + \mu_{HSO_4^-} \quad (2)$$

one can eliminate μ_{H^+} in Eq. (1) and obtain

$$2FE_j = \mu^{\epsilon}_A - \mu^{\delta}_A + 2\mu^{\delta}_{HSO_4^-} - 2\mu^{\epsilon}_{HSO_4^-} \quad (3)$$

The evaluation of the junction potential has been reduced to the evaluation of the difference of the electrochemical potential of the HSO_4^- ion throughout the junction, since μ_A is readily available in the literature [12]. We must now invoke the theory of transport in concentrated solutions in order to characterize the unknown electrochemical potential terms. Within the context of concentrated solution theory, a species flux is related to a linear combination of chemical-potential driving forces. In the absence of current, and for the case of the H_2SO_4 electrolyte in which bisulfate ion dissociation may be ignored, this theory [11] yields the result

$$\nabla\mu_{HSO_4^-} = t^0_{H^+}\nabla\mu_A \quad (4)$$

The above equation may be integrated to obtain

$$\mu^{\delta}_{HSO_4^-} - \mu^{\epsilon}_{HSO_4^-} = \int_{\epsilon}^{\delta} t^0_{H^+} d\mu_A \quad (5)$$

which allows Eq. (3) to be written as

$$2FE_j = \mu^{\epsilon}_A - \mu^{\delta}_A + 2\int_{\epsilon}^{\delta} t^0_{H^+} d\mu_A \quad (6)$$

Using the relations $t^0_{H^+} + t^0_{HSO_4^-} = 1$ and $d\mu_A = RT\, d\ln a_A$, we can write the final expression for the liquid-junction potential as

$$FE_j = \int_{\delta}^{\epsilon}\left(t^0_{HSO_4^-} - \frac{1}{2}\right)d\mu_A = RT\int_{\delta}^{\epsilon}\left(t^0_{HSO_4^-} - \frac{1}{2}\right)d\ln a_A \quad (7)$$

Since $t^0_{HSO_4^-} < 1/2$ in our concentration range of interest [5] and μ_A increases monotonically with increasing m_A, Eq. (7) tells us that $E_j < 0$ for the case in which solution ϵ is more concentrated than solution δ. Furthermore, for a junction defined by a typical RE composition of 6 *m* and an average cell composition at the end of discharge of 1 *m*, we can show that E_j is not negligible. For a simple estimate, we can define

an average transference number $\bar{t}^0_{HSO_4^-}$ and Eq. (7) can be approximated by

$$E_j \approx \frac{RT}{F}\left(\bar{t}^0_{HSO_4^-} - \frac{1}{2}\right)\ln\left(\frac{a^\epsilon_A}{a^\delta_A}\right) \quad (8)$$

Ref. [13] gives $a^\epsilon_A = 11.48\ m$ and $a^\delta_A = 7.164 \times 10^{-3}\ m$ and with an average transference number value of $\bar{t}^0_{HSO_4^-} = 0.23$ [5] we estimate a junction potential of -51 mV for this case. Clearly, liquid-junction potentials should be considered prior to the interpretation of experimental data.

3.2. Thermodynamic half-cell potentials with liquid junctions

We will now examine the thermodynamics of liquid-junction potential corrections for our two half-cells[2] (i.e., whether the E_j correction is added to or subtracted from a measurement of electrode potential relative to the Hg/Hg_2SO_4 RE). In the next section we will discuss the more realistic case of a half-cell in which there is the current flow between the Pb and PbO_2 electrodes and the cell acid composition may vary with time and position. Let us first examine a cell with a $Pb/PbSO_4$ electrode and the RE: cell II.

$$|Pb|PbSO_4|H_2SO_4^\delta \text{ in } H_2O|\text{junction}|H_2SO_4^\epsilon \text{ in } H_2O|Hg_2SO_4|Hg|$$

The thermodynamic open-circuit potential of this cell may be expressed as

$$2FE = \mu^\circ_{Pb} - \mu^\circ_{PbSO_4} - 2\mu^\circ_{Hg} + \mu^\circ_{Hg_2SO_4} + \mu^\delta_{HSO_4^-} - \mu^\epsilon_{HSO_4^-} + \mu^\epsilon_{H^+} - \mu^\delta_{H^+} \quad (9)$$

which may also be written as

$$E = E^\theta + E_j \quad (10)$$

when one recognizes the liquid-junction potential as defined by Eq. (1). The subtraction of the standard reduction potential of the $Pb/PbSO_4$ electrode from that of the Hg/Hg_2SO_4 electrode yields $E^\theta = 0.9718$ V [5]. The similar stoichiometries of the RE and the Pb electrode result in the absence of concentration dependent terms that are present in the PbO_2 half-cell potential expression. Of course, the correction of PbO_2-electrode potential measurements must be equal and opposite to that of the Pb electrode since the voltage difference between the two electrodes must be the same whether a liquid-junction potential exists or not. In the Appendix we develop analytical expressions for $t^0_{H^+}$ and a^δ_A as functions of m_A which are required to easily evaluate Eq. (7). Newman [11] gives a plot from which E, E^θ, and E_j versus m_A may be obtained. Our method is different only in that it is analytical. A purely analytical method can be more easily interfaced with a data acquisition system to give both corrected and uncorrected potential measurements as output.

At this point we would like to mention the luxury of a single electrolyte in the calculation of liquid-junction potentials. For the single electrolyte, the transference number and activity are functions only of the electrolyte concentration. For the case of two or more electrolytes, the integral of the transference number (see Eq. (7)) depends on the composition of more than one electrolyte and therefore a detailed knowledge of the composition profiles in the junction region is required [11].

3.3. Dynamic half-cell potentials with liquid junctions

Along with Eq. (7), Eq. (10) characterizes the half-cell potential of the Pb electrode in the absence of current. For the case with current flow between the Pb and PbO_2 electrodes during charge or discharge, we can write

$$E^{meas}_{PbO_2} = E^{corr}_{PbO_2} + E_j \quad (11)$$

for the PbO_2-electrode half-cell potential. The Pb-electrode half-cell corresponds to cell II with the electrodes reversed, therefore

$$E^{meas}_{Pb} = E^{corr}_{Pb} - E_j \quad (12)$$

In both of these equations, Eq. (7) can still be used to evaluate E_j since there is negligible current flow between working and reference electrodes — an ideal RE will not introduce any charge-transfer or ohmic overpotential into the half-cell potential measurement. The half-cell measurement, E^{meas}, includes the important charge-transfer overpotential information of the working electrode as well as other contributions such as ohmic potential drop. In the interest of eliminating from E^{meas} only sources of overpotential that are associated with the RE, we will further define E_j for a practical system as the potential arising from a liquid-junction region existing within the reference electrode. This junction region extends from the solution in contact with the mercury pool (ϵ) to the tip of the modified RE capillary connection that contacts solution at a particular point in the cell (δ). In the dynamic situation, H_2SO_4 concentration nonuniformities which occur within the cell constitute internal junction regions. However, since we wish only to remove sources of overpotential associated with the RE, the potentials of these internal junctions should not be eliminated from E^{meas}. The use of Eq. (7) to calculate E_j therefore requires knowledge of the ϵ and δ compositions. The reference composition (ϵ) is simple to evaluate experimentally since the RE compartment is external to the cell. However, since the H_2SO_4 concentration within the cell during discharge or charge is generally a function of position as well as time, evaluation of cell composition at the tip of the RE capillary (δ) is not as straightforward. If the cell composition were uniform during charge or discharge and only a function of time, then the δ composition could be estimated with a simple H_2SO_4 material balance. The initial H_2SO_4 concentration can be related to estimates of the initial molality and density with[3]

[2] The half-cell consists of the cell formed by the RE and either the Pb and PbO_2 electrode.

[3] Consistent units for this equation are c°_A in mol/cm^3, ρ° in g/cm^3, and m°_A in mol/g.

$$c_A^o = \frac{\rho_i^o m_A^o}{1 + M_A m_A^o} \tag{13}$$

For the case of constant current with only the discharge or charge reaction (i.e., no overcharge or self discharge) occurring within the cell, the average acid molality in the cell at any time during operation can be determined from the initial compositions and solution volumes, the current, and the cell stoichiometry

$$m_A(t) = \frac{\dfrac{V_i^o c_A^o}{A(N-1)} - \dfrac{it}{F}}{\dfrac{V_i^o c_A^o}{A(N-1)m_A^o} - M_{H_2O}\dfrac{it}{F}} \tag{14}$$

where V_i^o is the total cell initial liquid volume, N is the number of Pb and PbO_2 electrodes in the cell, and A is the geometric area of each electrode. This method of estimating the cell composition at the tip of the RE applies rigorously for the case of very low rates of discharge or charge. For example in Ref. [13] model cell calculations indicated nearly uniform H_2SO_4 concentration throughout the cell for charge at 3 mA/cm^2. The discharge and charge rates of 12.7 and 7.6 mA/cm^2, respectively, were investigated here, and the composition at the tip of the reference electrode contacting the top margins of the separators was taken to be the average composition given by Eq. (14). Open-circuit half-cell potential measurements of the Pb electrode at the end of discharge that are discussed in the next section confirm the use of Eq. (14) for the cell composition at the RE tip. Note that for very high current density operation in which the tip contacts a glass-mat type separator, the tip composition, and therefore E_j, should be essentially constant. In Ref. [14], model cell calculations indicated a nearly constant composition at the center of the separator for discharge at 400 mA/cm^2 while the composition within the electrodes varied significantly.

To summarize, the integral, Eq. (7), with d ln a_A as the integrand (and Eq. (A5) for transference number, in the Appendix) can be evaluated numerically with relative ease to obtain the liquid junction potential. As shown in the Appendix, the ln a_A increment can be evaluated with Eqs. (A3) and (A4), where the cell molality at a given time may be estimated with Eqs. (13) and (14). Eqs. (11) and (12) were used to obtain the corrected data for the PbO_2 and Pb half-cell potentials, respectively, given in the results section. The relevant cell characteristics are given in Table 1.

In our case, rather than calculate values of E_j separately for charge, we recognized that estimation for E_j depends only on the state-of-charge; the values calculated for discharge apply during charge at the corresponding state-of-charge. Since the acid concentration in the reference compartment is normally not far from the cell composition at the beginning of discharge, evaluation of the integral can be simplified.

Finally, we note that the transference number t_{H+}^0 for bulk H_2SO_4 in our liquid-junction potential calculations may not characterize the transport through the 50 Å diameter, glass-lined pores of the Vycor® material. There is evidence, however, of the applicability of macroscopic transport theory in inert porous materials with even smaller effective pore diameters [15].

4. Results and discussion

4.1. Half-cell potentials during discharge

The PbO_2 and Pb electrode half-cell potentials of a VRLA cell during a discharge (after 100 charge/discharge cycles) are shown in Fig. 2. The cell voltage at any time is indicated by the difference between the two half-cell potentials. The solid curves represent the raw experimental data. The dotted curves show the data with the liquid-junction potential eliminated according to the procedure given in Section 3. As the cell is discharged, the disparity in acid concentration between the cell and the reference compartment widens, which results in an increasing liquid-junction potential. Clearly, this potential is important in the interpretation of these experimental results. For example, without considering the liquid-junction potential, one might conclude that the Pb electrode is polarized about 100 mV during discharge, when actually the polarization is less than half that amount. Our estimate of the liquid-junction potential at the end of discharge was confirmed by open-circuit half-cell potential measurements of the Pb electrode. For example, after 94 min of discharge at cycle 162, we measured the Pb electrode half-cell potential at open circuit to be -0.918 ± 0.001 V. Eq. (12) can be used to estimate $E_j = -0.972\,V + 0.918\,V = -0.054$ V. This compares favorably to our calculation of E_j shown in Fig. 2 at 94 min of -0.056 V. It should also be mentioned that this open-

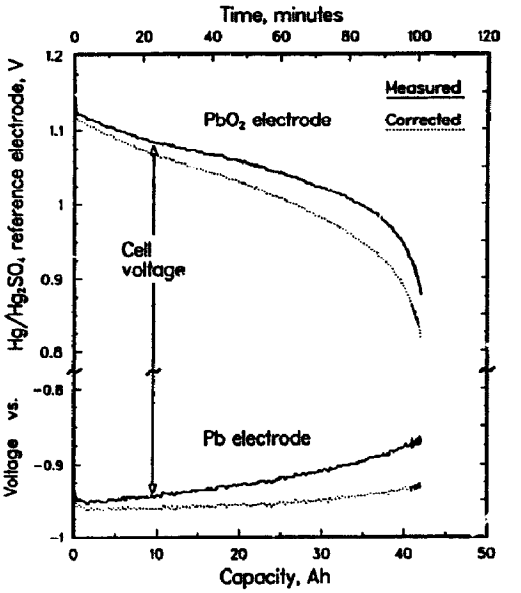

Fig. 2. Positive and negative electrode potentials vs. Hg/Hg_2SO_4 during the discharge portion of cycle 100. The solid and dotted curves, respectively, represent raw experimental data and those data after elimination of the liquid-junction potential.

circuit method is not suited to the PbO_2 electrode half-cell since this electrode equilibrates so slowly [5]. In contrast, Pb electrodes typically attain the thermodynamic half-cell potential of 0.972 V (at 25 °C) to within a few mV almost immediately after current interruption. Note that the good agreement between the measured and calculated liquid-junction potential indicates that the concentration of the solution in the separator margin that contacts the RE tip is close to the average concentration given by Eq. (14).

Focusing then on the corrected potential traces in Fig. 2, we see that the Pb half-cell potential trace is relatively flat throughout the discharge. The rapid decrease in the PbO_2 electrode potential near the end-of-discharge results in a similar decrease in cell voltage to the 1.75 V end-of-discharge value. In summary, the cell voltage alone cannot indicate which electrode limits discharge. Furthermore, only after accounting for the liquid-junction potential can one see that the capacity of the cell is almost exclusively limited by the positive electrode.

At the relatively low discharge rate studied here, ohmic and electrochemical kinetic resistances are unlikely to be significant. We believe the depletion of sulfuric acid within the PbO_2 electrode pores, much like that observed in the modeling work of Ref. [14], is a likely explanation for the capacity limitation.

4.2. Recharge behavior

Fig. 3 shows current, cell potential, and gas flow rates from the cell vent during the charge that followed the discharge depicted in Fig. 2. Fig. 4 shows the corresponding half-cell potentials (both measured and corrected). Perhaps the most

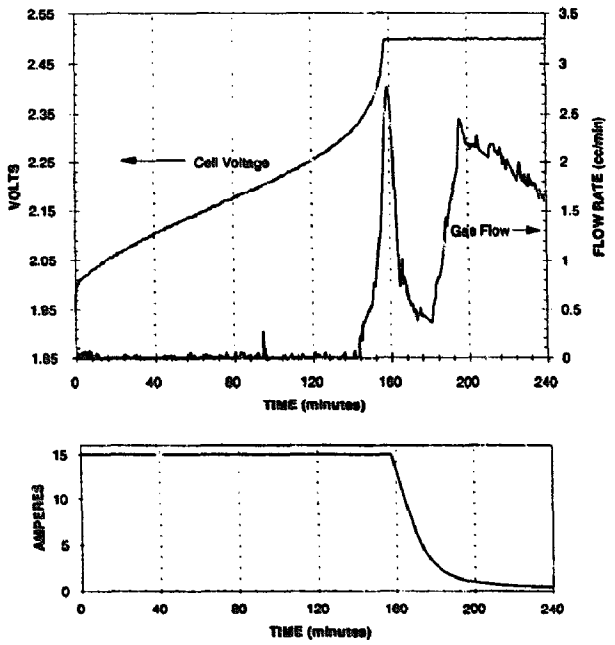

Fig. 3. Cell voltage and rate of vented gas (top panel) and cell current (bottom panel) during the charge portion of cycle 100.

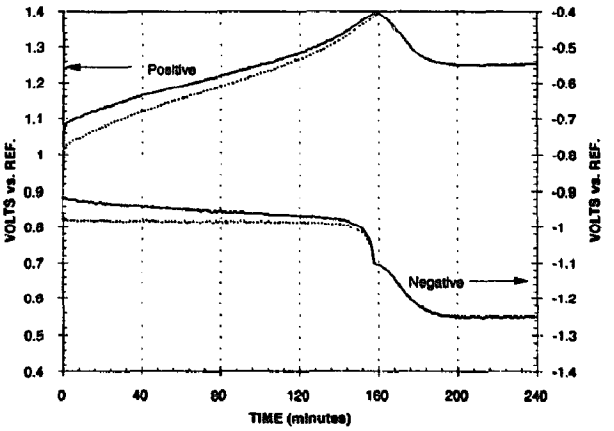

Fig. 4. Electrode potentials vs. Hg/Hg_2SO_4 during the charge portion of cycle 100. The solid and dotted curves, respectively, represent raw experimental data and those data after elimination of the liquid-junction potential.

striking feature of this data is the two gas flow peaks that occur during the latter portion of the charge. A comparison of these peaks to the half-cell potentials is illuminating. There is a close correlation between the location of the first flow peak (at nearly 160 min) and the location of the potential maximum exhibited by the PbO_2 electrode. At 143 min, the vent first releases gas, which indicates that the pressure within the cell has exceeded approximately 1 psig. Only after accounting for the liquid-junction potential can one see that the Pb half-cell potential has not varied significantly in these 143 min, which indicates that this electrode has been content to charge, rather than gas. It is the PbO_2 electrode that is being driven deeper and deeper into the potential region for oxygen evolution. This along with the observation that the gas flow decreases when the PbO_2 half-cell potential decreases (after the lid is reached) suggests that oxygen evolution at the PbO_2 electrode is largely responsible for the first gassing peak. Subsequent gas composition measurements taken from a similar cell support this view. The second region of significant gas flow is attributed to hydrogen evolution at the Pb electrode since the flow occurs as the Pb electrode reaches its highest polarization.

The half-cell polarization data also show the interplay between the electrode potentials that occurs to maintain the 2.5 V cell voltage lid, which is imposed experimentally. Before the voltage lid is reached, the polarization of the PbO_2 electrode is responsible for most of the relatively slow increase in cell voltage. In contrast, the final rapid increase in cell voltage is driven largely by a rapid polarization of the Pb electrode. It is interesting to note that once the cell voltage lid is reached, although the current is reduced to maintain the lid, the Pb electrode continues to polarize (albeit at a reduced rate) to still more negative potentials. Given this continued polarization of the Pb electrode, the PbO_2 electrode potential is forced to decrease the same amount to maintain a 2.5 V cell potential. Thus, use of a charge-voltage lid causes the PbO_2 electrode potential to go through a maximum.

It should be noted that our method of estimating the liquid-junction potential correction is subject to additional uncertainty near the end-of-charge when significant overcharge reactions such as oxygen evolution occur: Eq. (14) applies when only the overall cell reaction occurs. Eq. (14) could be extended to account for the overcharge reactions by including their current fractions, although such current-fraction information is not easily obtained. Fortunately, this uncertainty is of little consequence in our measurements since the liquid-junction potential is small at the end of charge when the average acid concentration in the cell approaches that in the reference compartment.

4.3. Conclusions

The RE described here performed admirably throughout the several months of testing a VRLA cell. The acid-starved nature of VRLA systems makes the inclusion of liquid-junction potential corrections particularly important in the analysis of the potential data obtained using this RE. The estimates of liquid-junction potential corrections can be confirmed by open-circuit measurements of Pb-electrode half-cell potentials. If one is primarily concerned about a particular region of charge (or discharge), then the acid concentration in the reference electrode can be tailored to minimize the corrections in the state-of-charge window of interest.

The polarization of the PbO_2 electrode was shown to control the decrease in cell voltage during discharge; that is, discharge capacity was limited at the PbO_2 electrode for the VRLA cell. During galvanostatic charge to a charge-voltage lid, the polarization of the PbO_2 electrode exhibited a maximum as a result of a large, rapid polarization of the Pb electrode. This potential maximum apparently caused a corresponding maximum in the rate of oxygen evolution at the PbO_2 electrode.

5. List of symbols

a_i	activity of species i, mol/kg
A	superficial electrode area, cm^2
c_i	concentration of species i, mol/cm^3
E	thermodynamic open-circuit potential, V
E_j	junction-potential difference (see Eq. (7)), V
F	Faraday's constant, 96 487 C/equiv
i	superficial current density, A/cm^2
I	total cell current, A
m_i	molality of species i, mol/kg
M_i	molecular weight of species i
N	number of electrodes in a cell stack
R	universal gas constant, 8.3145 J/(K mol)
t_i^0	transference number of species i relative to the solvent (species 0)
t	time, s
T	absolute temperature, K
V_l	total liquid solution volume within the cell, cm^3
$\bar{V}_i$	partial molar volume of species i, cm^3/mol

5.1. Greek letters

δ	cell H_2SO_4 composition in contact with the RE tip
ϵ	H_2SO_4 composition in contact with the RE mercury pool
μ_i	electrochemical or chemical potential of species i, J/mol
ρ_l	density of liquid H_2SO_4 solution, g/cm^3
θ	infinite dilution reference state for ions in solution

5.2. Subscripts and superscripts

avg	average
A	H_2SO_4
corr	corrected
0	species 0, the solvent water
l	liquid phase
meas	measured
Pb	Pb electrode
o	initial, prior to discharge or charge and pure phase
PbO_2	PbO_2 electrode

6. Appendix

6.1. Expressions for sulfuric acid activity and transference number

In order to estimate the liquid-junction potential with Eq. (7), we must have convenient expressions for a_A and t_{H+}^0 in terms of electrolyte composition. In the literature, these data are generally available in tabular form; however, analytic expressions are more convenient for use in computer code. For the cell III

$$|Pb|PbSO_4|H_2SO_4 \text{ in } H_2O|PbSO_4|PbO_2|$$

Bode[5] cites the expression

$$E = 1.9228 + 0.147519 \log m_A + 0.063552 \log^2 m_A + 0.073772 \log^3 m_A + 0.033612 \log^4 m_A \quad \text{(A1)}$$

for the thermodynamic open-circuit potential as a function of sulfuric acid molality at 25 °C. In terms of activities, we can write [12]

$$E = 2.048 + \frac{RT}{F} \ln\left(\frac{a_A}{a_{H_2O}}\right) \quad \text{(A2)}$$

The combination of Eq. (15) and Eq. (16) results in

$$\ln a_A = \frac{F}{RT}(-0.1252 + 0.147519 \log m_A + 0.063552 \log^2 m_A + 0.073773 \log^3 m_A + 0.033616 \log^4 m_A + \ln a_{H_2O}) \quad \text{(A3)}$$

Since the tabulated activity data in Ref. [12] indicate that the chemical potential of the acid dominates over that of the water in our composition range of interest, the $\ln a_{H_2O}$ term in the above equation is small relative to the other terms — a very accurate estimate of a_{H_2O} is not necessary.

Pitzer et al. [16] provide analytic expressions based on the theories of statistical mechanics for the thermodynamic properties of the sulfuric acid/water system as a function of composition and temperature, including HSO_4^- dissociation. For the case of $m_{SO_4^{-2}} = 0$ at 25 °C their expression becomes

$$\ln a_{H_2O} = -2m_A M_{H_2O}(1 + m_A(0.2103 + 0.4711 \exp(-2m_A^{1/2}))) + 2m_A M_{H_2O} 0.39105\left(\frac{m_A^{1/2}}{1 + 1.2m_A}\right) \quad \text{(A4)}$$

Note that expressions for the temperature dependence of the coefficients in the above expression are also given in Ref. [16]. Although one may expect the above approximate expression to be most accurate at high values of m_A when bisulfate ion dissociation is less important, actually, Eq. (A4) best approximates $\ln a_{H_2O}$ at the low values of m_A, when $a_{H_2O} \rightarrow 1$. Even at higher values of m_A, $\ln a_A$ evaluated by Eq. (A3) is within 2% of tabulated values in the literature. For example, at $m_A = 6$ *m*, Eq. (17) (with Eq. (A4) for $\ln a_{H_2O}$) yields $\ln a_A = 2.48$; the complete expressions of Pitzer et al. [16] which includes HSO_4^- dissociation, yields 2.45. Bullock [12] reports a value of 2.44. In general, the above expression will introduce an uncertainty in the estimate of the liquid-junction potential of less than 1 mV. Eq. (A3) along with Eq. (A4) is used to obtain a_A in terms of molality, which in turn is used to evaluate the junction-potential integral (i.e., Eq. (7)).

The tabulated data of t_{H+}^0 for various values of m_A at 25 °C given by Bode [5] can be represented very accurately by

$$t_{H+}^0 = 0.824 - 0.016 m_A \quad \text{(A5)}$$

in the range of $1\ m < m_A < 5\ m$. For higher concentrations Eq. (A5) is still acceptable. For example at $m_A = 8$, this equation yields a value of t_{H+}^0 that is within 1% of the value given in Ref. [5].

Acknowledgements

We are grateful to DELPHI Energy and Engine Management Systems Division General Motors Corporation for providing the test cell.

References

[1] H. Dietz, M. Radwan, H. Döring and K. Wiesener, *J. Power Sources, 42* (1993) 89–101.
[2] J.A. Magyar, M.A. Kepros and R.F. Nelson, *J. Power Sources, 31* (1990) 93–106.
[3] J. Mrha, J. Jindra and M. Musilova, *J. Power Sources, 32* (1990) 303–312.
[4] B.K. Mahato, E.Y. Weissman and E.C. Laird, *J. Electrochem. Soc., 121* (1974) 13–16.
[5] H. Bode, translated by R.J. Brodd and Karl V. Kordesch, *Lead-Acid Batteries*, Wiley, New York, 1977, p. 93.
[6] D.J.G. Ives and G.J. Janz, *Reference Electrodes Theory and Practice*, Academic Press, New York, 1961.
[7] J.S. Symanski, B.K. Mahato and K.R. Bullock, *J. Electrochem. Soc., 121* (1988) 548–551.
[8] R.L. Galyen and M.K. Carpenter, *J. Power Sources, 53* (1995) 323–326.
[9] J. Newman and W. Tiedemann, *J. Electrochem. Soc., 140* (1993) 1961–1968.
[10] J.O. Howell (Bioanalytical Systems), personal communication, 1995.
[11] J. Newman, *Electrochemical Systems*, Prentice-Hall, Englewood Cliffs, NJ, 1991, p. 273.
[12] K.R. Bullock, *J. Power Sources, 35* (1991) 197–223.
[13] D.M. Bernardi and M.K. Carpenter, *J. Electrochem. Soc., 142* (1995) 2631–2642.
[14] T.B. Nguyen, R.E. White and H. Gu, *J. Electrochem. Soc., 137* (1990) 2998.
[15] M.W. Verbrugge and P.N. Pintauro, *Mod. Aspects Electrochem., 19* (1989) 24–25.
[16] K.S. Pitzer, R.N. Roy and L.F. Silvester, *J. Am. Chem. Soc., 99* (1977) 4930–4936.